

# Hole concentration and phonon renormalization in Ca-doped YBa<sub>2</sub>Cu<sub>3</sub>O<sub>y</sub> ( $6.76 \leq y \leq 7.00$ )

K. C. Hewitt

*Dalhousie University, Department of Physics,  
Halifax, Nova Scotia, Canada B3H 3J5\**

X. K Chen, C. Roch, J. Chrzanowski, J. C. Irwin  
*Simon Fraser University, Department of Physics,  
Burnaby, British Columbia, Canada, V5A 1S6*

E. H. Altendorf

*Microvision Inc., Bothell, Washington , USA 98011*

R. Liang, D. Bonn, W. N. Hardy

*University of British Columbia, Department of Physics,  
Vancouver, British Columbia, Canada V6T 1Z1*

(Dated: November 20, 2018)

## Abstract

In order to access the overdoped regime of the YBa<sub>2</sub>Cu<sub>3</sub>O<sub>y</sub> phase diagram, 2 % Ca is substituted for Y in YBa<sub>2</sub>Cu<sub>3</sub>O<sub>y</sub> ( $y = 7.00, 6.93, 6.88, 6.76$ ). Raman scattering studies have been carried out on these four single crystals. Measurements of the superconductivity-induced renormalization in frequency ( $\Delta\omega$ ) and linewidth ( $\Delta 2\gamma$ ) of the 340 cm<sup>-1</sup> B<sub>1g</sub> phonon demonstrate that the magnitude of the renormalization is directly related to the hole concentration ( $p$ ), and not simply the oxygen content. The changes in  $\Delta\omega$  with  $p$  imply that the superconducting gap ( $\Delta_{max}$ ) decreases monotonically with increasing hole concentration in the overdoped regime, and  $\Delta\omega$  falls to zero in the underdoped regime. The linewidth renormalization  $\Delta 2\gamma$  is negative in the underdoped regime, crossing over at optimal doping to a positive value in the overdoped state.

PACS numbers: 74.25.Gz, 74.25.Jb, 74.25.Kc, 74.62.Dh, 74.72.Bk

## I. INTRODUCTION

Certain phonons in cuprate superconductors exhibit anomalous changes in frequency and linewidth when they are cooled through the superconducting transition temperature. Such phonon anomalies were first discovered in High Temperature Superconductors (HTS) by Macfarlane *et al*<sup>1</sup> in  $\text{YBa}_2\text{Cu}_3\text{O}_{7-\delta}$  (Y123). Zeyher and Zwicknagl<sup>2,3</sup> showed that the presence of such anomalies could be attributed to electron-phonon interactions and the changes in the density of electronic states that occur on the opening of the superconducting gap. Friedl *et al*<sup>4</sup> used this approach to obtain an estimate for the superconducting gap in Y123. Nicol, Jiang and Carbotte<sup>5</sup> extended the theoretical approach of Zeyher and Zwicknagl to include the effect of a pairing interaction of d-wave symmetry on the phonon self-energy. Phonon anomalies have been investigated extensively, using Raman scattering, in several cuprates -  $\text{YBa}_2\text{Cu}_3\text{O}_{7-\delta}$ <sup>6,7,8,9,10,11</sup>,  $\text{YBa}_2(\text{Cu}_{1-x}\text{M}_x)_4\text{O}_8$  (Y124) for  $\text{M}=\text{Zi}, \text{Mn}$ <sup>12</sup>,  $\text{Bi}_2\text{Sr}_2\text{CaCu}_2\text{O}_{8+\delta}$ (Bi2212)<sup>13,14</sup>,  $\text{NdBa}_2\text{Cu}_3\text{O}_{7-\delta}$  (Nd123)<sup>15</sup>,  $\text{HgBa}_2\text{Ca}_2\text{Cu}_3\text{O}_{8+\delta}$  (Hg1223)<sup>16</sup>,  $\text{HgBa}_2\text{Ca}_3\text{Cu}_4\text{O}_{10+\delta}$  (Hg1234)<sup>17</sup>,  $\text{HgBa}_2\text{CuO}_{4+\delta}$  (Hg1201)<sup>18</sup> and  $(\text{Cu},\text{C})\text{Ba}_2\text{Ca}_3\text{Cu}_4\text{O}_x$ <sup>19</sup>. In particular, many studies have been carried out on the  $340\text{ cm}^{-1}$   $\text{B}_{1g}$  phonon in Y123 to ascertain the nature of the phonon anomaly. At this time, however, the reason for the sensitivity of the  $\text{B}_{1g}$  phonon anomaly to extremely small changes in the oxygen content near optimal doping remains somewhat controversial<sup>20,21</sup>. Additionally, the physical basis of the relationship between hole concentration and the degree of phonon renormalization is unclear.

Subsequent to the early experiments<sup>1,4</sup> it was found<sup>6,7,22</sup> that the strength of the renormalization is very sensitive to the presence of small amounts of impurities, even in crystals for which the critical temperature remained close to the maximum value of 93.5 K. For example the anomaly is very weak in samples containing a small percentage of either Thorium<sup>6,7</sup> or Gold<sup>22</sup>, where Th substitutes for Yttrium, and Au for Cu(1). To explain this effect it was initially suggested that the presence of impurities led to the averaging of an anisotropic gap<sup>23</sup>.

It was also known<sup>24</sup> that the strength of the  $\text{B}_{1g}$  phonon anomaly is very weak in samples of Y-123 with a reduced oxygen concentration ( $y < 6.90$ ), and, in particular<sup>9</sup> the strength of the anomaly is very sensitive to oxygen content near optimal doping. For example it is very weak in crystals with  $y < 6.90$  and  $T_c = 92\text{K}$ , weak in crystals with  $y = 6.95$  and

$T_c = 93.7$  K, and yet very strong in overdoped crystals with  $y = 7.0$  and  $T_c = 89.5$  K. In view of the fact that small changes in oxygen doping produced the same effects as small changes in impurity concentrations it was suggested<sup>7,9</sup> that the strength of the  $B_{1g}$  anomaly is determined by the free carrier, or hole concentration, in the  $\text{CuO}_2$  planes. This suggestion was supported by the observation<sup>25</sup> that the frequency of the pair-breaking peak in the  $B_{1g}$  electronic Raman continuum is very sensitive to the level of oxygen doping and, furthermore, that its behavior could be correlated with the strength of the phonon anomaly. That is, the variation of the frequency of the  $B_{1g}$  pair breaking peak with doping, moved in complete step with the value of the gap obtained from an analysis of the phonon anomaly. The dependence on hole concentration has been revisited in a recent examination of Ca - doped Y-123<sup>26</sup>.

In an attempt to gain additional insight into the above question, and into the origin of the physical processes that determine the sensitivity of the  $B_{1g}$  phonon anomaly to doping, we have carried out Raman scattering investigations of Ca-doped Y-123 ( $\text{Y}_{1-x}\text{Ca}_x\text{Ba}_2\text{Cu}_3\text{O}_y$  or Y(Ca)-123). Calcium, a divalent alkaline-earth ion, substitutes preferentially for trivalent Yttrium in the  $\text{YBa}_2\text{Cu}_3\text{O}_y$  compound. Since the ionic radius of the  $\text{Ca}^{2+}$  ion is approximately equal to that of the  $\text{Y}^{3+}$  ion<sup>27</sup> one expects that the carrier or hole concentration could be varied in a controlled manner without introducing any significant distortion in the Y-123 lattice<sup>28</sup>. Also, given that the Y-site is located midway between the superconducting  $\text{CuO}_2$  planes, Ca substitution should be an effective means of increasing the carrier concentration on the  $\text{CuO}_2$  planes. On the basis of simple valence considerations one might thus expect that each substituted Ca ion would contribute 0.5 holes to each  $\text{CuO}_2$  plane<sup>28,29</sup>. Although this recipe appears to break down in the case of more heavily doped samples<sup>30</sup> ( $x > 0.1$ ), the results presented here, which were obtained using relatively lightly doped ( $x = 0.02$ ), high-quality single crystals of Y(Ca)-123, appear to be in accord with these expectations. Our results indicate that the effect of calcium doping on the  $B_{1g}$  phonon anomaly is equivalent in every way to the changes induced by appropriate variation of the oxygen concentration. That is, the magnitude of the renormalization is directly related to the hole concentration, in contrast to recent observations<sup>26</sup>. In addition, it is found that the superconductivity induced (SCI) frequency renormalization is small for  $p < 0.15$ , increases rapidly just above optimum doping, and then increases monotonically with increasing hole concentration (for  $p > 0.15$ ). The SCI linewidth renormalization changes from a narrowing below optimal to a broadening above. These results are consistent with the absence of a SCI electronic renormalization in

the underdoped state where a pseudogap opens above  $T_c$ .

## II. SAMPLE PREPARATION & CHARACTERIZATION

Good quality  $Y_{1-x}Ca_xBa_2Cu_3O_y$  (Y(Ca)-123) crystals were grown in yttrium-stabilized zirconia crucibles ( $ZrO_2$ -Y) by a standard flux method<sup>31</sup>. Based on stoichiometry considerations the [Ca] was estimated to be 4%, but Inductively-Coupled Mass Spectrometry (ICPMS) analysis<sup>32</sup> yielded a lower value of  $2.0 \pm 0.2$  %.

An estimate of the oxygen content ( $y_{est}$ ) was obtained using the crystal growth parameters of annealing pressure and temperature<sup>33</sup>. To determine the values of  $y$  more accurately, the c-axis lattice parameter was carefully measured by X-ray diffraction (XRD) studies. Using a Siemens D-5000 diffractometer with Cu- $K_\alpha$  radiation, XRD patterns were obtained using scans with a step size  $\Delta\theta = 0.02^\circ$ , in the range  $5^\circ \leq 2\theta \leq 100^\circ$ . In order to obtain reliable estimates of the c-axis lattice parameter only the (00 $l$ ) peaks with  $2\theta > 30^\circ$  ( $l > 5$ ) were used in a nonlinear least-squares fit to the diffraction peaks. The refinement program corrects for off-axis shifts and consequently the c-axis spacings reported in Table I are accurate to within  $\pm 0.002$  Å.

In agreement with expectations<sup>28</sup>, as mentioned above, it was found that the c-axis lattice parameter is not affected by small concentrations of Ca. Therefore, using the relation between the c-axis length and the oxygen concentration<sup>9</sup>, more accurate values for the oxygen concentrations ( $y_{ref}$ ) were obtained (see Table I). The samples of 2 % Ca-doped Y123 are therefore labeled according to their oxygen concentration ( $y = 7.00$ (A), 6.93(B), 6.88(C), 6.76(D)), and an undoped sample ( $y = 6.93$  (U)) is also used for comparison purposes. The critical temperature,  $T_c$ , was obtained from DC magnetization measurements as described elsewhere<sup>31</sup>.

The relationship between the oxygen concentration and hole carrier content ( $p$ ) in the crystals was deduced using a modified form of a relation proposed by Tallon<sup>35</sup>. He proposed that  $p = 0.187 - 0.21(7-y)$ , where  $p$  is the number of holes per  $CuO_2$  layer and  $y$  is the oxygen concentration. In this work, however, we will use a slightly displaced value of the p-intercept to be consistent with an optimum hole concentration of 0.16, which is obtained when  $y = 6.93$  and  $T_{c,max} = 93.7$ K. Accordingly,

$$p = 0.175 - 0.21(7 - y) \tag{1}$$

The critical temperatures of the samples, as a function of the hole concentration per  $\text{CuO}_2$  ( $p$ ), follow the parabolic dependence (Fig. 1) reported in other papers<sup>30,35</sup>,

$$T_c/T_{c,max} = 1 - 82.6(p - p_o)^2 \quad (2)$$

where  $p_o = 0.16$  is the optimum hole concentration at  $T_{c,max}$ .

It can be seen from Fig. 1 that crystal C is optimally doped, D is underdoped and A and B are overdoped. We can conclude that 2% Ca-doping of the Y-123 crystals does not involve any noticeable oxygen depletion, which has been reported<sup>27,30,36,37</sup> to occur for Ca concentrations greater than 10%. Consequently, the substitution of Calcium (+2) for Yttrium (+3) effectively increases the hole concentration as  $p = p^* + [\text{Ca}]/2$ , where  $p^*$  would be the hole concentration in Ca-free material. As one can conclude from an inspection of Table I, only sample A exhibits  $y_{est} < y_{ref}$ , which may suggest that the sample is oxygen depleted. However, since sample D is the only underdoped crystal, further investigations are necessary to validate this conclusion.

### III. RAMAN SPECTRA

Raman spectra of the Y(Ca)-123 crystals were collected using either the 514.5 nm or 488.0 nm lines of an argon-ion laser as the excitation source. To minimize local heating effects, the incident power was kept below 3 mW, and focussed on the sample with a spherical-cylindrical lens combination to yield incident power densities of the order  $10\text{W}/\text{cm}^2$ . With this incident power level the local sample heating is minimal. This is clear from the fact that the observed renormalizations occur very close to the measured critical temperatures. Spectra were obtained at various temperatures in the range  $15\text{K} < T < 300\text{K}$ , using a Displex refrigerator. All the sample temperatures cited in this paper are the measured ambient temperatures.

Within the  $D_{4h}$  point group, excitations of  $B_{1g}$  symmetry are selected by using, in Porto's notation, the  $z(x'y')z$  scattering geometry, where  $x'$  denotes the (1,1,0) direction,  $y'$  denotes the (-1,1,0) direction and  $z$  is the direction parallel to the  $c$ -axis. In this geometry the (1,0,0) and (0,1,0) axes lie along the Cu-O bonds. The scattered light was analyzed with a triple-grating spectrometer, using gratings with a bandpass of either  $700\text{ cm}^{-1}$  or  $1400\text{ cm}^{-1}$ . The corresponding resolution at the detector is  $0.8$  or  $1.6\text{ cm}^{-1}$ , respectively. The scattered light

is detected by an ITT-Mepsicron imaging detector over a typical collection time of 1 hour. The spectra were carefully calibrated against the laser plasma lines.

$B_{1g}$  spectra were obtained at several different temperatures for all samples. Spectra at 16.6 K from sample A is shown in Fig. 2. Quantitative analysis of the linewidth ( $2\gamma = \Gamma$ ) and frequency ( $\omega_o$ ) of this mode was carried out by fitting the lineshapes to Fano profiles<sup>38</sup> with a linear plus constant background ( $b\omega + c$ ):

$$I(\omega) = I_o \frac{(q + \epsilon)^2}{1 + \epsilon^2} + b\omega + c \quad (3)$$

where,

$$I_o = \pi \rho_o T_e^2 \quad (4)$$

$$\epsilon = \frac{(\omega - \omega_o)}{\gamma} \quad (5)$$

$$\gamma = \pi \rho_o V^2 \quad (6)$$

$$q = \frac{T_p}{\pi \rho_o V T_e} \quad (7)$$

Here we assume a constant density of electronic states over the energy range of interest ( $\rho_o$ ),  $V$  measures the interaction between phonon and electronic continuum states, and  $T_e$ ,  $T_p$  are the matrix elements characterizing Raman-active transitions to the electronic continuum and phonon states, respectively.  $\gamma$  is the half-width-at-half-maximum (HWHM) of the lineshape and  $q$  is the asymmetry parameter which determines the form of the lineshape, while  $b$  and  $c$  are adjustable constants. An example of the results of such a fit is shown in Fig. 2.

The temperature dependence of the frequency ( $\omega_o$ ) and linewidth ( $2\gamma = \text{FWHM}$ ) of the  $340 \text{ cm}^{-1}$   $B_{1g}$  Raman mode are summarized in Figs. 3 and 4, respectively. As can be seen from these figures, the (nominal)  $340 \text{ cm}^{-1}$   $B_{1g}$  mode clearly shows significant changes in linewidth and frequency as a function of temperature.

As seen in Fig. 3, the magnitude of the phonon *frequency* decreases substantially in crystals with lower oxygen content. The renormalization is largest<sup>39</sup> in the highly oxygenated samples and almost vanishes in the sample with an oxygen content  $y = 6.76$ . There is also a substantial softening of the phonon below 100 K, by  $11 \text{ cm}^{-1}$  in crystals with the highest oxygenation. This softening approximately scales with the oxygen content and in crystals with  $y = 6.76$  the softening is reduced to about  $2\text{-}3 \text{ cm}^{-1}$ .

The *linewidth* of the  $340 \text{ cm}^{-1}$  peak (Fig. 4) decreases when cooled between room temperature and 10 K. To determine the superconductivity induced changes one must subtract

anharmonic effects. To obtain a rough estimate of the anharmonic changes that occur one can assume that the phonon decays into two phonons with opposite  $q$  vector, each having a frequency  $\omega_o/2$ . The temperature dependence of the linewidth can then be described approximately by the anharmonic decay equation<sup>4,40,41</sup>,

$$\Gamma_{AH}(\omega_o, T) = c[1 + 2n(\omega_o/2, T)] + d \quad (8)$$

where  $n$  is the Bose-Einstein factor,  $c$  and  $d$  are constants, and  $\omega_o$  is the frequency of the mode. Since the Bose factor is relatively constant for temperatures below 100K (for  $\omega_o > 300\text{cm}^{-1}$ ), anharmonic effects should be negligible for the  $340\text{ cm}^{-1}$  phonon in the range  $100\text{K} > T > 15\text{ K}$ . The constants  $c$  and  $d$  can thus be determined by fitting to the linewidth changes that occur for  $T > 100\text{K}$ , and the resulting equation can be used to predict the anharmonic behaviour that occurs below 100K. The superconductivity induced changes are then assumed to be the actual linewidth minus that predicted by the anharmonic equation. These changes are strongly dependent on the oxygen content. In the crystals with very high oxygenation ( $y = 6.98\text{-}7.00$ ), there is a pronounced broadening ( $4\text{ cm}^{-1}$  for sample A) of the peak. In samples (C & D) with the lowest oxygen concentration ( $y = 6.88$  and  $6.76$ ), a  $2\text{-}3\text{ cm}^{-1}$  step-like narrowing is observed below 80 K without any initial broadening. In the crystal (B) possessing an intermediate oxygen content ( $y = 6.93$ ), after an initial broadening ( $1\text{ cm}^{-1}$ ) below 100 K, a narrowing takes place below 50 K ( $0.5\text{ cm}^{-1}$ ).

In order to quantify the SCI changes in frequency and linewidth and to facilitate comparison with the results<sup>8</sup> obtained from Ca-free crystals, the procedures used in Ref.<sup>4,8</sup> will be applied to the results shown in Figs. 3 and 4. That is, the magnitude of the frequency anomaly is estimated by finding the difference in the frequency of the phonon at two temperatures. Quantitatively, for a given doping level, the magnitude of the phonon frequency anomaly ( $\Delta\omega$ ) is determined by the difference in the phonon frequency at 30 K and 100 K,

$$\Delta\omega \equiv \omega(30K) - \omega(100K),$$

Fig. 4 shows that as the sample is cooled below  $T_c$  the linewidth departs from the anharmonic decay curve. The phonon linewidth anomaly ( $\Delta 2\gamma$ ) is measured at the temperature  $T_o$  ( $< T_c$ ) where the deviation reaches its maximum. It's magnitude is defined as the difference between the linewidth at  $T_o$  and the value calculated from anharmonic decay of the phonon at the same temperature,

$$\Delta 2\gamma \equiv 2\gamma(T_o) - \Gamma_{AH}(T_o)$$

where,  $\gamma_{AH}$  is the anharmonic linewidth given by equation 8.

When  $\Delta 2\gamma$  and  $\Delta\omega$  are plotted as a function of hole concentration (Fig. 5), a number of features are evident. First, the Ca-free and 2 % Ca-doped crystals fall on the same curve. If the [Ca] were ignored, the corresponding points in Fig. 5 would be shifted (by 0.01) to lower hole concentrations, and consequently they would not fall on the same curve as the Ca-free crystals. This observation allows one to conclude that it is the change in hole concentration that is the determining factor - independent of whether it is determined by oxygen or Ca doping.

Secondly, the most pronounced broadening ( $\Delta 2\gamma = 4\text{cm}^{-1}$ ) and softening ( $\Delta\omega = 11\text{cm}^{-1}$ ) of the  $340\text{ cm}^{-1}$  mode occurs for the sample (A) with the highest hole concentration, estimated to be  $p = 0.185$  (Table I). In fact, Fig. 5 demonstrates that the magnitude of the frequency renormalization monotonically increases as the hole concentration is increased. According to theory<sup>2,3</sup>, as the superconducting gap energy, or the pair-breaking peak in the electronic continuum, approaches the  $340\text{ cm}^{-1}$  phonon frequency from above, the phonon damping and frequency renormalization should markedly increase, as is observed. Our results thus imply that for optimal doping,  $2\Delta > \omega_o = 340\text{ cm}^{-1}$ , and that the superconducting gap decreases with increasing doping in overdoped crystals. In fact Bock et al<sup>42</sup>, in thin films with much higher Ca concentrations, carried out measurements on samples with  $2\Delta < \omega_o$ . They found that  $2\Delta = \omega$  for a sample with  $p \approx 0.20$ .

#### IV. DISCUSSION AND CONCLUSIONS

Substituting Ca for Y in  $\text{YBa}_2\text{Cu}_3\text{O}_y$  ( $6.85 \leq y < 7$ ) has allowed us to access the overdoped regime of Y123. The superconductivity induced renormalization of the  $340\text{ cm}^{-1}$   $B_{1g}$  phonon has been studied as a function of oxygen concentration in both in pure and in Ca-doped crystals. In overdoped compounds the strength of the phonon anomaly increases as the doping level is increased above optimum ( $p = 0.16$ ). This is consistent with the known behaviour of the superconducting gap. In optimally doped compounds the  $B_{1g}$  pair breaking peak is centered at approximately  $550\text{ cm}^{-1}$  ( $2\Delta = 8.4\text{kT}$ ) and this decreases to  $470\text{ cm}^{-1}$  ( $2\Delta \approx 7.5\text{kT}$ ) for a crystal with  $p$  approx 0.18 (Fig 1). Thus the gap energy is approaching the phonon frequency from above and the increase in strength of the phonon anomaly is completely consistent with the predictions of Zeyher and Zwicky<sup>2,3</sup>. The results presented



here demonstrate that the behaviour in high quality crystals containing 2% Ca is identical to that observed in undoped samples with the same hole concentration. These conclusions are corroborated by the results of measurements<sup>42</sup> carried out on high quality thin films of Ca-doped Y123. In that work it was found that  $2\Delta \approx 340 \text{ cm}^{-1}$  for  $p$  approx 0.20. This variation in the gap energy with hole concentration, in the overdoped regime, is very similar to that found in Bi2212<sup>43</sup> and La214<sup>44</sup>.

As noted above, the frequency shift associated with the phonon anomaly undergoes rather dramatic changes as the doping level moves through optimum. From Fig. 5 one can see that for  $p = 0.185$ , a doping level slightly above optimum,  $\Delta\omega \approx 12 \text{ cm}^{-1}$ .  $\Delta\omega$  then decreases quite rapidly to  $\Delta\omega \approx 4 \text{ cm}^{-1}$  at optimum ( $p_o = 0.16$ ). As the doping level is reduced below optimum  $\Delta\omega$  decreases more gradually, and reaches a value ( $\approx 2 \text{ cm}^{-1}$ ) that is comparable to the experimental uncertainty when  $p \approx 0.14$ . The SCI linewidth change  $\Delta 2\gamma$ , on the other hand, is even more dramatic in that it abruptly changes from a positive value to a negative value (Fig. 5) as the doping level is reduced through optimum. These results suggest that the electron phonon interaction decreases rapidly as the doping level is reduced through the optimum value. This can be attributed to a corresponding decrease in the carrier concentration, and thus the results are consistent with investigations<sup>44</sup> which show that the pseudogap opens abruptly, and the  $B_{1g}$  spectral weight decreases dramatically, as the doping level in Y123 is reduced below  $p_o$ . The absence of a phonon frequency anomaly, and a narrowing of the linewidth, are thus completely consistent with this picture<sup>44,45,46</sup> of the pseudogap. The results also suggest that Ca- doping does not influence the onset of the pseudogap, and again, in high quality samples, the pseudogap opens at a particular hole concentration, irrespective of how it is generated.

It is also interesting to note that the SCI renormalization of the  $B_{1g}$  electronic continuum in Y123 and La214 also vanishes<sup>25</sup> rather abruptly as the doping level is reduced below optimum, and its doping dependence has been found<sup>25</sup> to be closely correlated with that of the phonon anomaly. This is in contrast to results obtained in Bi2212<sup>43</sup> where it is found that a SCI renormalization of the  $B_{1g}$  electronic continuum is observed well into ( $p \approx 0.12$ ) the underdoped region. This result has been attributed<sup>43</sup> to an inherent inhomogeneity in Bi2212; that is, in the underdoped material, Bi2212 is composed of underdoped and optimally doped regions. Given the absence of any strong variations in behaviour of specific heat measurements<sup>47,48</sup> near optimum doping one might speculate that a similar inhomogeneity

might be present in  $Y_{1-x}Ca_xBa_2Cu_3O_y$  for samples with  $x \geq 0.10$ .

## V. ACKNOWLEDGEMENTS

The financial support of the Natural Sciences and Engineering Research Council of Canada is gratefully acknowledged.

- 
- \* Electronic address: Kevin.Hewitt@Dal.ca; URL: <http://fizz.phys.dal.ca/~hewitt>
- <sup>1</sup> R. M. Macfarlane, H. J. Rosen, and H. Seki, *Solid State Commun.* **63**, 831 (1987).
  - <sup>2</sup> R. Zeyher and G. Zwicknagl, *Solid State Commun.* **66**, 617 (1988).
  - <sup>3</sup> R. Zeyher and G. Zwicknagl, *Z. Phys. B- Condensed Matter* **78**, 175 (1990).
  - <sup>4</sup> B. Friedl, C. Thomsen, and M. Cardona, *Phys. Rev. Lett.* **65**, 915 (1990).
  - <sup>5</sup> E. J. Nicol, C. Jiang, and J. P. Carbotte, *Phys. Rev. B* **47**, 8131 (1993).
  - <sup>6</sup> E. Altendorf, J. C. Irwin, W. N. Hardy, and R. Liang, *Physica C* **185-189**, 1375 (1991).
  - <sup>7</sup> E. Altendorf, J. Chrzanowski, J. C. Irwin, A. O. O'Reilly, and W. N. Hardy, *Physica C* **175**, 47 (1991).
  - <sup>8</sup> E. Altendorf, J. C. Irwin, R. Liang, and W. N. Hardy, *Phys. Rev. B* **45**, 7551 (1992).
  - <sup>9</sup> E. Altendorf, X. K. Chen, J. C. Irwin, R. Liang, and W. N. Hardy, *Phys. Rev. B* **47**, 8140 (1993).
  - <sup>10</sup> R. Hauff, S. Tajima, W. J. Jang, and A. I. Rykov, *Phys. Rev. Lett.* **77**, 4620 (1996).
  - <sup>11</sup> A. G. Panfilov, M. F. Limonov, A. I. Rykov, S. Tajima, and A. Yamanaka, *Phys. Rev. B* **57**, R5634 (1998).
  - <sup>12</sup> N. Watanabe and N. Koshizuka, *Phys. Rev. B* **57**, 632 (1998).
  - <sup>13</sup> D. H. Leach, C. Thomsen, and M. Cardona, *Solid State Commun.* **88**, 457 (1993).
  - <sup>14</sup> A. A. Martin, J. A. Sanjurjo, K. C. Hewitt, X.-Z. Wang, J. C. Irwin, and M. J. G. Lee, *Phys. Rev. B* **56**, 8426 (1997).
  - <sup>15</sup> O. V. Misochko, K. Kuroda, and N. Koshizuka, *Phys. Rev. B* **56**, 9116 (1997).
  - <sup>16</sup> X. Zhou, M. Cardona, D. Colson, and V. Viallet, *Phys. Rev. B* **55**, 12770 (1997).
  - <sup>17</sup> V. G. Hadjiev, X. Zhou, T. Strohm, M. Cardona, Q. M. Lin, and C. W. Chu, *Phys. Rev. B* **58**, 1043 (1998).

- <sup>18</sup> M. C. Krantz, C. Thomsen, H. Mattausch, and M. Cardona, Phys. Rev. B **50**, 1165 (1994).
- <sup>19</sup> V. G. Hadjiev and M. Cardona, TCSUH-preprint **97**, 137 (1997).
- <sup>20</sup> A. P. Litvinchuk, C. Thomsen, and M. Cardona, Solid State Commun. **83**, 343 (1992).
- <sup>21</sup> A. P. Litvinchuk, C. Thomsen, M. Cardona, L. Borjesson, P. Berastegui and L. -G. Johansson, Phys. Rev. B **50**, 1171 (1994).
- <sup>22</sup> K. F. McCarty, J. Z. Liu, Y. X. Jia, R. N. Shelton, and H. B. Radowsky, Physica C **192**, 331 (1992).
- <sup>23</sup> C. Thomsen, B. Friedl, M. Cieplak, and M. Cardona, Solid State Commun. **78**, 727 (1991).
- <sup>24</sup> M. Krantz, H. J. Rosen, R. M. Macfarlane, and V. Y. Lee, Phys. Rev. B **38**, 4992 (1988).
- <sup>25</sup> X. K. Chen, E. Altendorf, J. C. Irwin, R. Liang, and W. N. Hardy, Phys. Rev. B **48**, 10530 (1993).
- <sup>26</sup> J. W. Quilty and H. J. Trodahl, Phys. Rev. B **61**, 4238 (2000).
- <sup>27</sup> C. Greaves and P. R. Slater, Supercon. Sci. Tech. **2**, 5 (1989).
- <sup>28</sup> B. Fisher, J. Genossar, C. G. Kuper, L. Patlagan, G. M. Reisner, and A. Knizhnik, Phys. Rev. B **47**, 6054 (1993).
- <sup>29</sup> R. A. Gunasekaran, R. Ganguly, and J. V. Yakhmi, Physica C **243**, 160 (1995).
- <sup>30</sup> J. T. Kucera and J. C. Bravman, Phys. Rev. B **51**, 8582 (1995).
- <sup>31</sup> R. Liang, P. Dosanjh, D. A. Bonn, D. J. Barr, J. F. Carolan, and W. N. Hardy, Physica C **195**, 51 (1992).
- <sup>32</sup> Measurements made at **ALS Environmental**, 1988 Triumph Street, Vancouver, BC, Canada V5L 1K5, Tel: 604 253 4188.
- <sup>33</sup> P. Schleger, W. N. Hardy, and B. X. Yang, Physica C **176**, 261 (1991).
- <sup>34</sup> K. G. Vandervoort, U. Welp, J. E. Kessler, H. Claus, G. W. Crabtree, W. K. Kwok, A. Umezawa, B. W. Veal, J. W. Downey, A. P. Paulikas and J. Z. Liu, Phys. Rev. B **43**, 13042 (1991).
- <sup>35</sup> J. L. Tallon, C. Bernhard, H. Shaked, R. L. Hitterman, and J. D. Jorgensen, Phys. Rev. B **51**, 12911 (1995).
- <sup>36</sup> A. Manthiram and J. B. Goodenough, Physica C **159**, 760 (1989).
- <sup>37</sup> C. Gledel, J. F. Marucco, and B. Touzelin, Physica C **165**, 437 (1990).
- <sup>38</sup> M. V. Klein, in *Physical Properties of High Temperature Superconductors*, edited by D. M. Ginsberg (World Scientific, Singapore, 1989), Chap. 4, p. 171.
- <sup>39</sup> Actually, in the article of Altendorf *et al.* (1993)<sup>9</sup>, the broadening of the  $340 \text{ cm}^{-1}$  mode in their

most oxygenated sample ( $y=7$ ) is about twice that observed in our sample A ( $x=0.02,y=7$ ). The presence of potassium ( $K^+$ ) impurities in their sample is, at least, partly responsible, since the substitution of monovalent K for trivalent Y or divalent Ba would increase the hole concentration.

- <sup>40</sup> P. G. Klemens, Phys. Rev. **148**, 845 (1966).
- <sup>41</sup> D. A. Kleinman, Phys. Rev. **118**, 118 (1960).
- <sup>42</sup> A. Bock, S. Ostertun, R. Das Sharma, M. Rubhausen, K.-O. Subke, and C. T. Rieck, Phys. Rev. B **60**, 3532 (1999).
- <sup>43</sup> K. C. Hewitt and J. C. Irwin, Phys. Rev. B **66**, 054516 (2002).
- <sup>44</sup> J. C. Irwin, J. G. Naeini, and X. K. Chen, in *Doping Dependence of the Pseudogap in High Temperature Superconductors: A Raman study*, Vol. 27/28 of *Studies of High Temperature Superconductors*, edited by A. V. Narlikar (Nova Science Publishers, Commack, New York, 1999).
- <sup>45</sup> X. K. Chen, J. G. Naeini, J. C. Irwin, R. Liang, and W. N. Hardy, J. Phys. Chem. Solids **59**, 1968 (1998).
- <sup>46</sup> J. G. Naeini, X. K. Chen, J. C. Irwin, M. Okuya, T. Kimura, and K. Kishio, Phys. Rev. B **59**, 9642 (1999).
- <sup>47</sup> J. L. Tallon and J. W. Loram, Physica C **349**, 53 (2001)
- <sup>48</sup> J. L. Luo, J. W. Loram, J. R. Cooper, K. A. Mirza and D. Jin, Physica B **284**, **1045 (2000)**

TABLE I: Values of the initial oxygen concentration ( $y_{est}$ ) estimated from the crystal growth parameters. The refined oxygen concentration ( $y_{ref}$ ) calculated from the c-axis length.  $p$  is the hole concentrations calculated from the expression  $p = 0.175 - 0.21(7 - y)$  and  $p^* = p + [Ca]/2 = p + 0.01$ . Crystals A, B, C and D have  $[Ca] = 0.02$ , while crystal U is an undoped crystal used for comparison purposes.

Crystal	$y_{est}$	$c \pm 0.002$ (Å)	$y_{ref}$	$p_{ref}^*$	$p_{ref}$	$T_c$ (K)
A	6.98	11.688	7.00	0.175	0.185	89.5
B	6.95	11.698	6.93	0.161	0.171	92.0
C	6.90	11.707	6.88	0.149	0.159	92.7
D	6.85	11.725	6.76	0.125	0.135	89.5
U	6.95	11.699	6.93	0.160	0.160	93.2

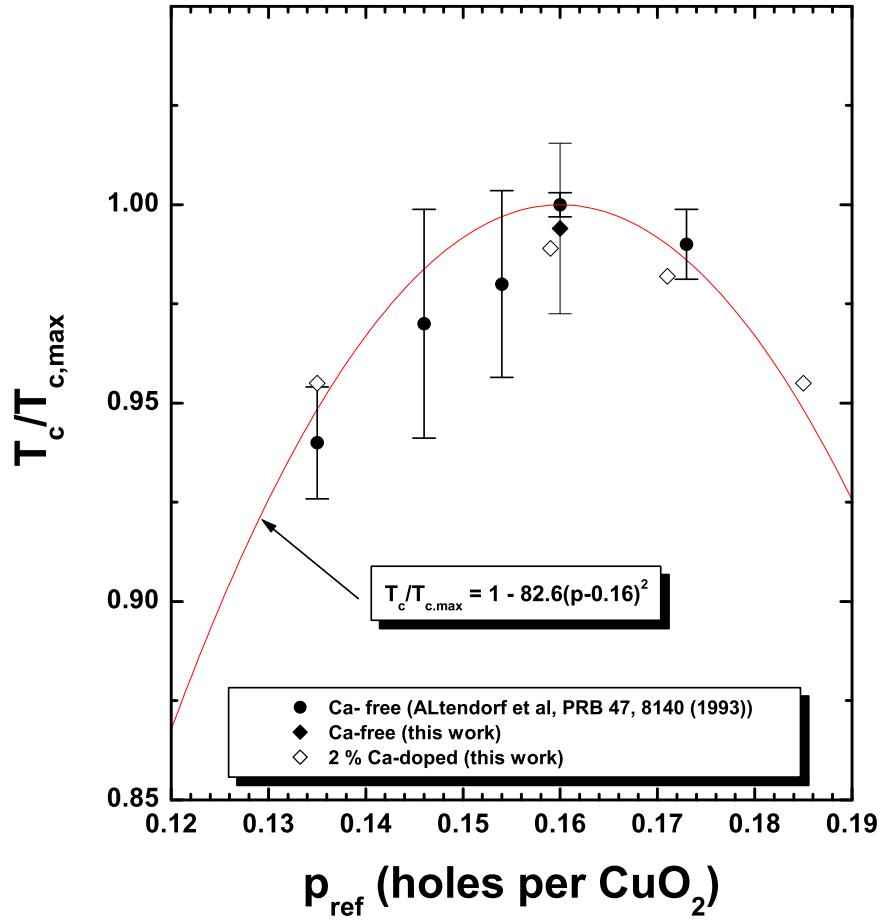


FIG. 1: The superconducting transition temperature versus hole concentration for Ca-doped (2%) and Ca-free crystals of Y123.

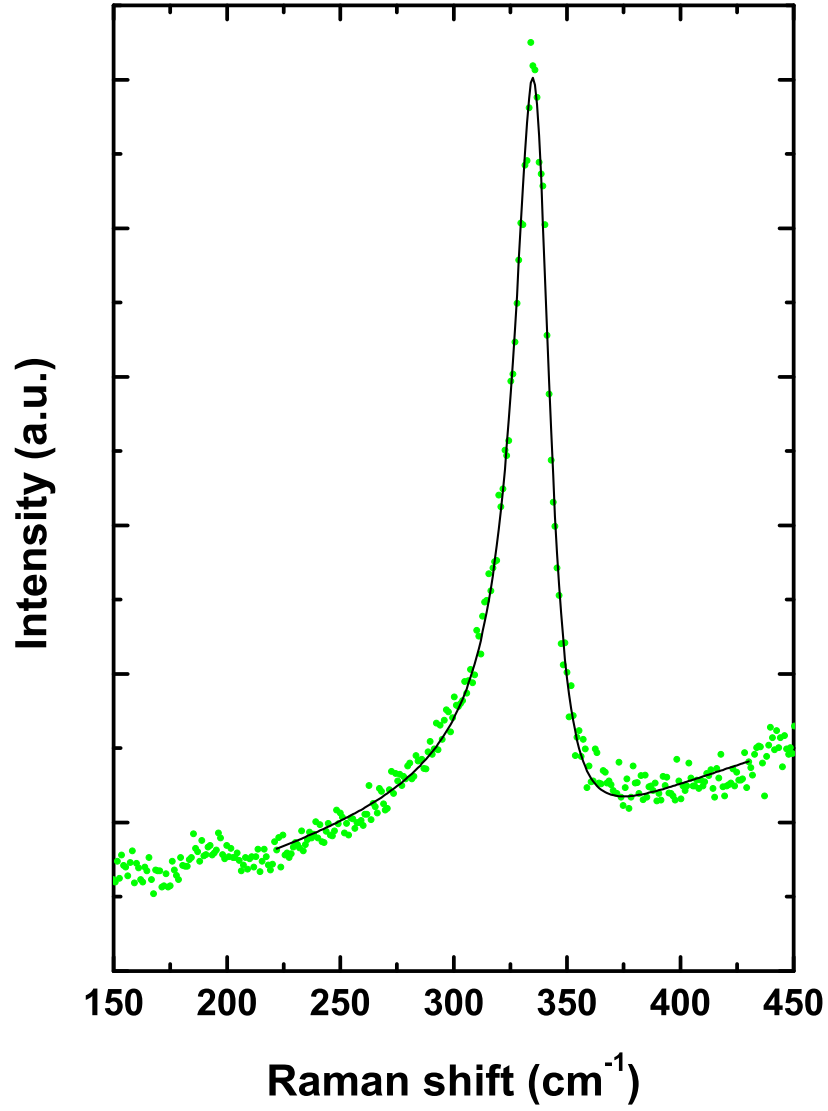


FIG. 2: Fano lineshape fit (solid line) to the (nominal)  $340 \text{ cm}^{-1}$  phonon found in the  $B_{1g}$  spectra (dots) of sample A at  $T = 16.6 \text{ K}$ , resulting in  $\omega = 336.3 \pm 0.1 \text{ cm}^{-1}$ ,  $q = -6.0 \pm 0.2$  and HWHM  $\gamma = 9.6 \pm 0.1 \text{ cm}^{-1}$ .

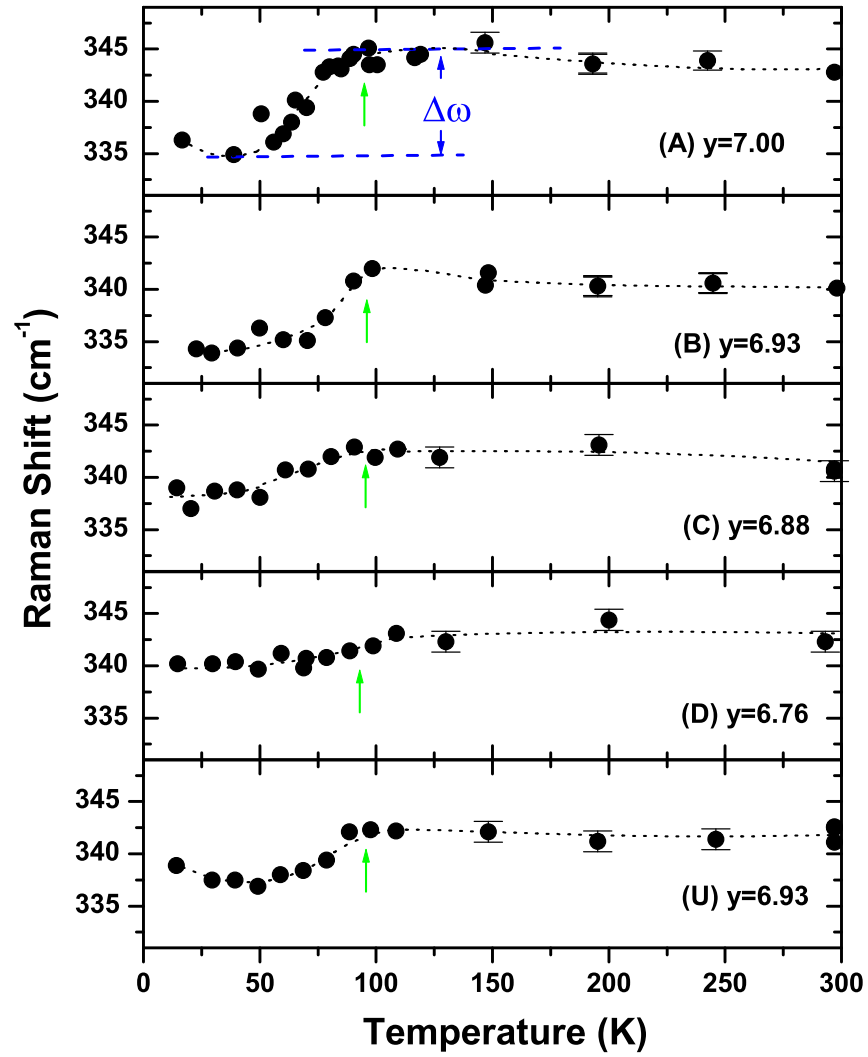


FIG. 3: The temperature dependence of the  $340 \text{ cm}^{-1}$  phonon frequency, for 2 % Ca-doped (A-D) and Ca-free (U) crystals with varying oxygen concentrations.



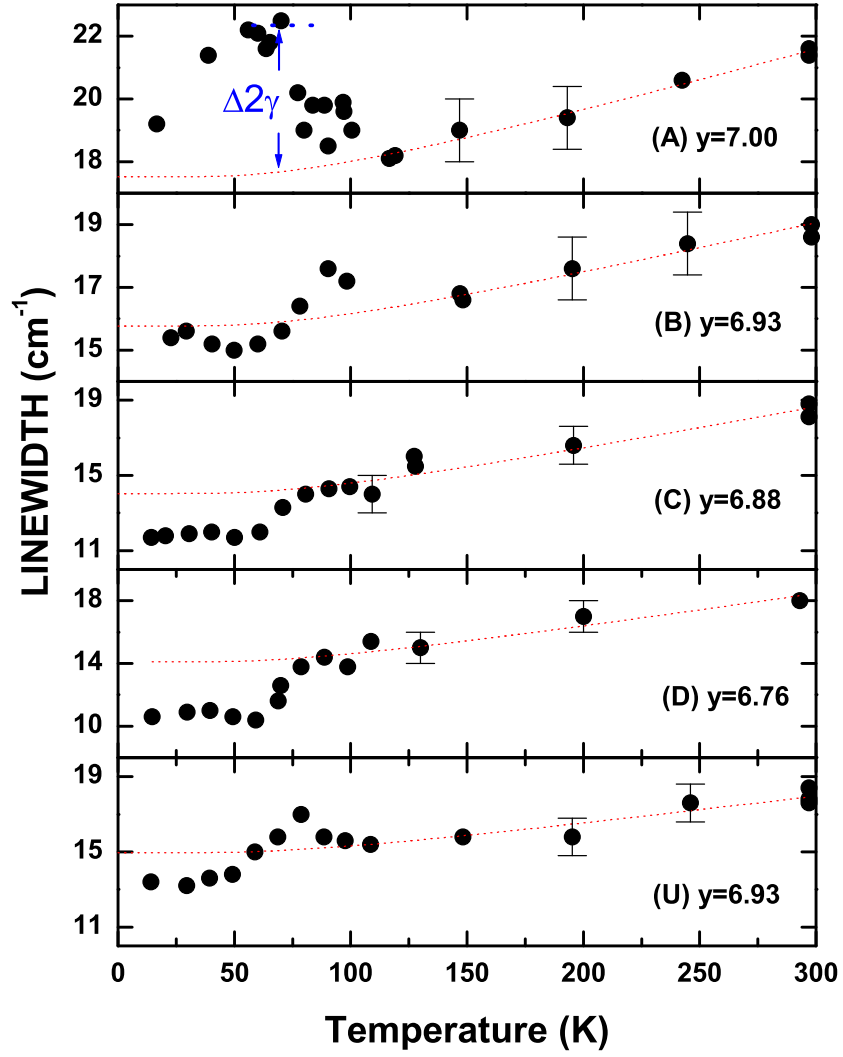


FIG. 4: The temperature dependence of the 340 cm<sup>-1</sup> B<sub>1g</sub> phonon linewidth for 2 % Ca-doped (A-D) and Ca-free (U) crystals with the indicated oxygen concentrations.

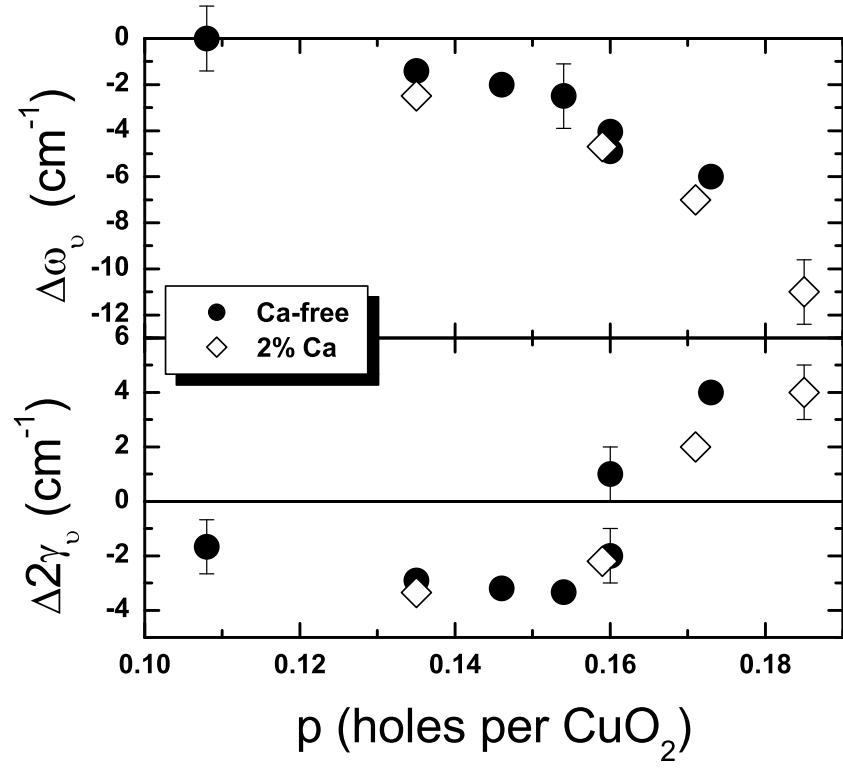


FIG. 5: Superconductivity induced renormalization in frequency and linewidth of the  $340 \text{ cm}^{-1}$   $B_{1g}$  mode, as a function of hole concentration in Y123.